

Experimental Status of Exotic Mesons and the GlueX Experiment

Daniel S. Carman

Jefferson Laboratory, Newport News, VA 23606

E-mail: carman@jlab.org

Abstract. One of the unanswered and most fundamental questions in physics regards the nature of the confinement mechanism of quarks and gluons in QCD. Exotic hybrid mesons manifest gluonic degrees of freedom and their spectroscopy will provide the data necessary to test assumptions in lattice QCD and the specific phenomenology leading to confinement. Within the past two decades a number of experiments have put forth tantalizing evidence for the existence of exotic hybrid mesons in the mass range below 2 GeV. This talk represents an overview of the available data and what has been learned. In looking toward the future, the GlueX experiment at Jefferson Laboratory represents a new initiative that will perform detailed spectroscopy of the light-quark meson spectrum. This experiment and its capabilities will be reviewed.

1. Motivation for the Study of Hybrid Mesons

High energy experiments have provided clear evidence for significant contributions of gluons to hadronic structure. Evidence for gluons has been found in jet measurements and deep inelastic scattering. However, descriptions of gluonic degrees of freedom in the low energy regime of soft gluons are still unavailable. This description is necessary to better understand the detailed nature of confinement. The nature of this mechanism is one of the great mysteries of modern physics, and in order to shed light on this phenomenon, we must better understand the nature of the gluon and its role in the hadronic spectrum. Confinement within the theory of strongly interacting matter, Quantum Chromodynamics (QCD), arises from the postulate that gluons can interact among themselves and give rise to detectable signatures within the hadronic spectrum. These signatures are expected within hadrons known as hybrids, where the gluonic degree of freedom is excited and can provide for a more detailed understanding of the confinement mechanism in QCD.

Gluonic mesons represent a $q\bar{q}$ system in which the gluonic flux-tube contributes directly to the quantum numbers of the state. In terms of the constituent quark model, the quantum numbers of the meson are determined solely from the quark and antiquark. However, QCD indicates that this simple picture is incomplete. Lattice QCD calculations predict that hybrid states with the flux-tube carrying angular momentum should exist, as well as purely gluonic states (called glueballs). Modern lattice calculations for mesons show that indeed a string-like chromoelectric flux-tube forms between distant static quark charges as shown in Fig. 1a. The non-perturbative nature of the flux-tube leads to the confinement of the quarks and to the well-known linear inter-quark potential from heavy-quark confinement with $dV/dr \sim 1 \text{ GeV/fm}$ (see

Fig. 1b). These calculations predict that the lowest lying hybrid meson states are roughly 1 GeV more massive than the conventional meson states. This provides a reference point for the mass range to which experiments must be sensitive.

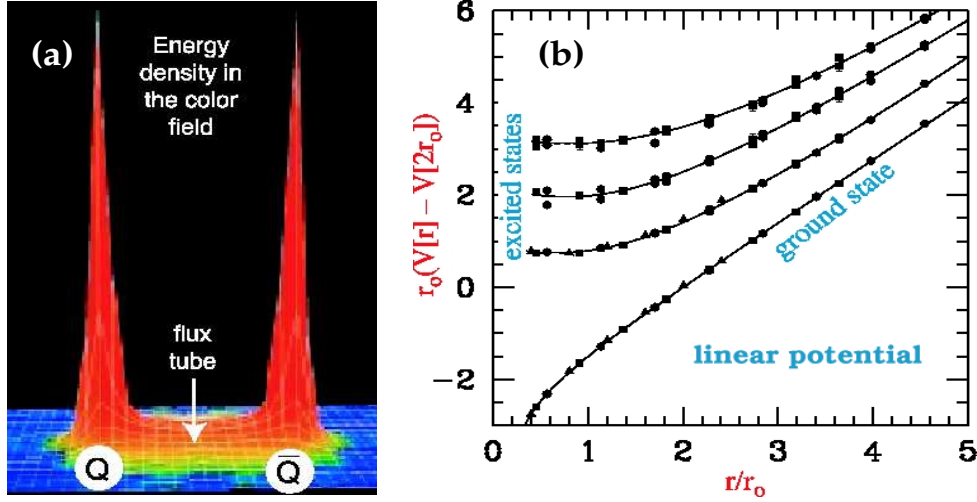


Figure 1. (a). A lattice QCD calculation of the energy density in the color field between a quark and an antiquark [1]. This density peaks at the locations of the q and \bar{q} and is confined to a flux-tube stretching between the pair. (b). Corresponding lattice calculation of the potential between the quarks showing the ground and low-lying excited states [2]. These calculations are for heavy quarks in the quenched approximation.

2. Hybrid Meson Properties

Within the standard non-relativistic constituent quark model, conventional mesons are made up from $q\bar{q}$ pairs with the spin 1/2 quarks coupled to a total spin $S=0$ or 1. These pairs are then coupled with units of orbital angular momentum L , and a possible radial excitation. The relevant quantum numbers to describe these states for a given principal quantum number n are J^{PC} , where $\vec{J} = \vec{L} + \vec{S}$ represents the total angular momentum, $P = (-1)^{L+1}$ represents the intrinsic parity, and $C = (-1)^{L+S}$ represents the C -parity of the state.

The light-quark mesons are built up from u , d , and s quarks and their antiquarks. For each value of S , L , and n , a nonet of mesons is expected for each value of J^{PC} . The lowest possible mass states for these conventional mesons (i.e. for $L=0$, $n=1$) are then $J^{PC} = 0^{-+}$ for $S=0$ (corresponding to the π , η , η' , and K mesons) and $J^{PC} = 1^{--}$ for $S=1$ (corresponding to the ρ , ω , ϕ , and K^* mesons). The lowest lying $S=0$ mesons have masses of about 500 MeV and the lowest lying $S=1$ mesons have masses of about 800 MeV. Nonets of higher mass mesons for a given principal quantum number are then built up by adding in units of L . Conventional mesons correspond to states with the flux-tube in its ground state, and as such, the gluonic degree of freedom does not contribute.

The hybrid meson quantum numbers can be predicted within the flux-tube model [3]. In its ground state, the flux-tube carries no angular momentum. The lowest excitation is an $L=1$ rotation which contains two degenerate states (corresponding to clockwise and counterclockwise rotations). Linear combinations of these states give rise to quantum numbers of $J^{PC} = 1^{-+}$ or 1^{+-} for the flux-tube. Adding these quantum numbers to those for the $q\bar{q}$ pair gives the possible J^{PC} for the hybrid mesons, which also are expected to have a nonet of states for each J^{PC} . For $S = L = 0$, the possible quantum numbers are $J^{PC} = 1^{--}$ and 1^{++} . Note that exotic hybrid mesons are *not* generated when $S=0$, as these quantum numbers are possible for conventional $q\bar{q}$ states such as ρ , ω , and ϕ . An important consideration in the study of these states is that

non-exotic hybrids may mix with conventional $q\bar{q}$ states making clear experimental identification difficult. Establishing the hybrid nonets will depend on starting with nonets whose quantum numbers are exotic to which ordinary $q\bar{q}$ states cannot couple.

For $S=1$, $L=0$ states the possible quantum numbers are $J^{PC} = 0^{+-}, 0^{-+}, 1^{-+}, 1^{+-}, 2^{+-}, 2^{-+}$. Of these states, those with $J^{PC} = 0^{+-}, 1^{-+}$, and 2^{+-} are manifestly exotic, i.e. they are not allowed for ordinary $q\bar{q}$ states. The existence of exotic hybrid mesons has been predicted for more than 3-decades. Almost all QCD models predict a $J^{PC} = 1^{-+}$ hybrid with a mass at or below 2 GeV [3, 4, 5, 6], with favored widths in the range $\Gamma \sim 40 \rightarrow 100$ MeV [7]. However, the decay modes are uncertain. In the flux-tube model, the gluonic excitation does not transfer its spin to the relative orbital angular momentum of the final state mesons, and hybrid decay to two mesons with quarks in S -waves does not occur [8]. However, other models predict such a decay, through effects such as spurious bag CM motion [5], or through the sequential decay of the exotic hybrid into a non-exotic hybrid and then into a conventional meson via mixing [9]. The non-exotic hybrid is mixed with a conventional meson which appears in the final state.

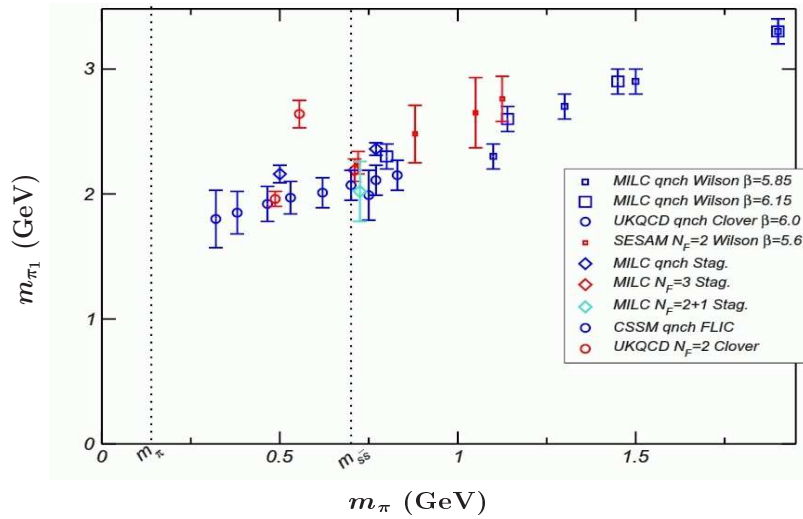


Figure 2. A survey of current LQCD results for the lightest $J^{PC} = 1^{-+}$ exotic plotting m_{π_1} vs. m_{π} . The open and closed symbols denote dynamical and quenched simulations, respectively.

A summary of current LQCD calculations for the lowest lying non-strange $J^{PC} = 1^{-+}$ exotic meson is provided in Fig. 2 [10, 11]. These quantum numbers should correspond to the lightest nonet. These calculations are quenched or partially quenched at the current time with some employing improved lattice actions, and they indicate that the rough mass scale to search in is about 1.5 - 2.0 GeV.

3. Experimental Status of $J^{PC}=1^{-+}$ Hybrids

While the current results from lattice QCD indicate that the lightest exotic meson nonet has quantum numbers $J^{PC}=1^{-+}$ and its lightest member, the π_1 , has a mass in the range from 1.5 to 2.0 GeV, the current experimental evidence is much less clear. During the past two decades, a number of different experiments have provided tantalizing evidence for the 1^{-+} exotics $\pi_1(1400)$, $\pi_1(1600)$, and $\pi_1(2000)$. If each of these states was verified, this would result in an overpopulation of the 1^{-+} hybrid nonet where there should be only one π_1 state. In this section I provide a brief overview on each of the reported 1^{-+} exotic candidates.

Beyond issues associated with the statistics in each of these analyses, the different experiments are hampered by a number of analysis issues. Perhaps the most important arises due to leakage effects in the amplitude analysis. While the implementation of a partial wave analysis is in

principle straightforward, there are difficulties that arise due to the detector system employed, as well as ambiguities within the partial wave analysis (PWA) framework itself. Effects such as detector acceptance and resolution can conspire to allow strength from a dominant partial wave to appear as strength in a weaker wave. Another important issue involves the model-dependent assumptions made within the PWA framework itself. In PWA, simplifying assumptions are used in order to make the fitting model more tractable, such as in calculating decay amplitudes via an isobar model, and the absolute effects of these assumptions are not fully known.

3.1. Evidence for the $\pi_1(1400)$

The $\pi_1(1400)$ was first reported by the GAMS group at CERN [12]. It was seen in the $\pi^-p \rightarrow \eta\pi^0n$ channel at $p_\pi=100$ GeV. A partial wave analysis of these data showed a clear $a_2(1320)$ D -wave, and a narrow enhancement in the unnatural parity exchange P_0 -wave at a mass of ~ 1.4 GeV. The natural parity exchange P_+ -wave was observed structureless. However, these conclusions were refuted by some of the original authors who pointed out that the $\eta\pi^0$ PWA suffered from an eight-fold ambiguity which was not properly accounted for in the analysis [13, 14]. The VES Collaboration at IHEP [15], which studied the reaction $\pi^-N \rightarrow \pi^-\eta N$ with $p_\pi=37$ GeV, reported a small but statistically significant broad enhancement in the natural parity exchange P_+ -wave at about 1.4 GeV. The authors did not identify the P_+ enhancement as a resonance. Experiment E179 at KEK studied the decay angular distributions in the $\pi^-p \rightarrow \eta\pi^-p$ reaction at $p_\pi=6.3$ GeV. They observed an enhancement around 1.3 GeV in the P_+ -wave but were unable to establish a resonant nature. They noted the phase of the P_+ -wave relative to the D_+ $a_2(1320)$ wave showed no distinct variation with mass [16].

The first resonant claim of the $\pi_1(1400)$ was provided by the E852 Collaboration at BNL in the reactions $\pi^-p \rightarrow \eta\pi^0n$ and $\pi^-p \rightarrow \eta\pi^-p$ at $p_\pi=18$ GeV [17]. In this analysis the resonant nature of the P_+ -wave arises from a strong interference with the D_+ $a_2(1320)$ wave. The phase difference between these waves exhibited a phase motion not attributable solely to the $a_2(1320)$. Results from the Crystal Barrel experiment at CERN for the reactions $\bar{p}p \rightarrow \eta\pi^0\pi^0$ and $\bar{p}n \rightarrow \eta\pi^-\pi^0$ at $p_{\bar{p}}=200$ MeV [18], needed to include a $\pi_1(1400)$ state in addition to conventional mesons to fit their data.

In the PDG listings [19], the mass of the $\pi_1(1400)$ is $M=1376\pm 17$ MeV and its width $\Gamma=300\pm 40$ MeV with observed decays to $\eta\pi^0$ and $\eta\pi^-$. However the current experimental evidence gives rise to a number of controversial issues. The $\pi_1(1400)$ is significantly lighter than theoretical expectations, and its only observed decay mode into $\eta\pi$ is not expected (or strongly disfavored) for a gluonic hybrid. It has been suggested that the $\pi_1(1400)$ could represent a meson-meson molecule. An alternative suggestion is that the $\pi_1(1400)$ could actually be a threshold effect of a higher mass π_1 resonance due to the opening of more favorable decay channels. Other recent work suggests that the exotic P -wave signature for the $\pi_1(1400)$ may actually arise from dynamical non-resonant scattering, similar to S -wave $\pi\pi$ scattering at low energy [20].

A recent analysis of E852 data by Dzierba *et al.* focussed on an amplitude analysis of the $\eta\pi^0$ mode in three different t bins (see Fig. 3) [21]. This analysis concluded that no consistent P -wave resonant parameters can describe the data for the $\pi_1(1400)$, while the resonant parameters obtained for the $a_2(1320)$ phase reference state are consistent for the different t bins with the PDG values. However the question remains as to what causes the peaking in the P -wave intensity distributions, and if it is due to a non-resonant source, what explains the phase motion with respect to the $a_2(1320)$?

Another interesting fact is that while the exotic wave is a few percent of the dominant a_2 wave in the E852 data, it is of comparable strength to the a_2 in the Crystal Barrel results. However, each of the existing data sets in these hadroproduction experiments is hampered by relatively low statistics.

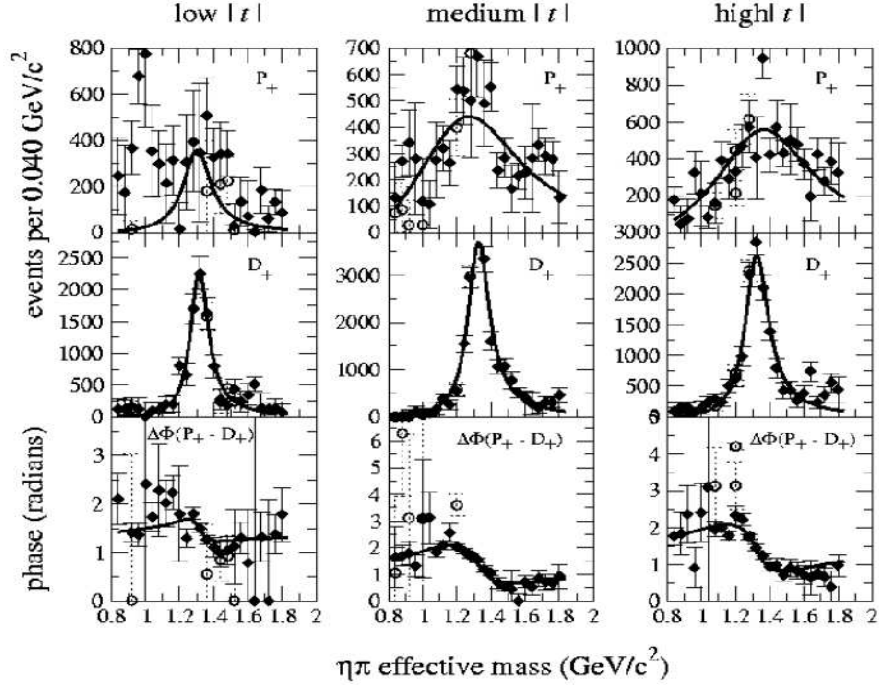


Figure 3. PWA solution for the P_+ (top) and D_+ (middle) waves, and the phase difference (bottom) for the three t bins used in the analysis as a function of the $\eta\pi^0$ effective mass [21].

3.2. Evidence for the $\pi_1(1600)$

A second $J^{PC} = 1^{-+}$ exotic meson at 1.6 GeV has been claimed by the BNL E852 Collaboration in the $\eta'\pi$, $\rho\pi$, $b_1\pi$, and $f_1\pi$ final states in π^-p reactions at $p_\pi=18$ GeV [22, 23, 24, 25]. This signal first appeared as an enhancement in the P_+ -wave in an early $\eta'\pi$ measurement by the VES Collaboration [15]. Additional VES measurements followed with confirmation of the $\pi_1(1600)$ decaying into $b_1\pi$, $\eta'\pi$, and $\rho\pi$ [26]. This work provided measurements of the relative branching ratios into $b_1\pi$, $\eta'\pi$, and $\rho\pi$ of 1.0:1.0:1.6. These predictions are highly at odds with predictions of the flux-tube model. Thus either these three modes are not all due to a hybrid meson or there is a problem with the amplitude analysis or the flux-tube model.

The evidence for the $\pi_1(1600)$ from its decay into $\rho\pi$ is particularly controversial. The analysis results for the $\rho\pi$ final state are shown in Fig. 4. The top row of this figure shows the $\rho\pi$ analysis from E852 [22] from the 1994 data run based on 250k events. Here an exotic 1^{-+} signal is reported at a mass of $M=1593\pm 8$ MeV with a width $\Gamma=168\pm 20$ MeV. The middle (bottom) row of Fig. 4 shows analysis of the 1995 E852 data by Dzierba *et al.* [27] for $\rho\pi$ decay to $\pi^-\pi^-\pi^+$ ($\pi^-\pi^0\pi^0$). This later data run had roughly four times the statistics compared to the earlier run, and highlighted a strong PWA model dependence of the shape and magnitude of the 1^{-+} signal. The 1^{-+} intensity distribution exhibits a strong resonance-like distribution using a PWA model with a minimum number of partial waves (21 waves). However, when a larger wave set is used (denoted as the high wave set in Fig. 4 – includes 35 waves), the evidence for the $\pi_1(1600)$ in the intensity distributions is washed out. Nonetheless, it is curious that the phase motion plots are essentially unchanged between the two choices of wave sets. The comparison of the two $(3\pi)^-$ modes provides powerful cross checks on the analysis results. Any resonance decaying to $(\rho\pi)^-$ should decay equally to $(\pi^-\pi^0)\pi^0$ and $(\pi^+\pi^-)\pi^0$, and thus appear with equal probabilities in the two modes.

In the E852 analysis of $\pi^-p \rightarrow \eta'\pi$, evidence for an exotic 1^{-+} state with a mass $M=1597\pm 10$ MeV and width $\Gamma=340\pm 40$ MeV is shown [23] (see Fig. 5). It is interesting that

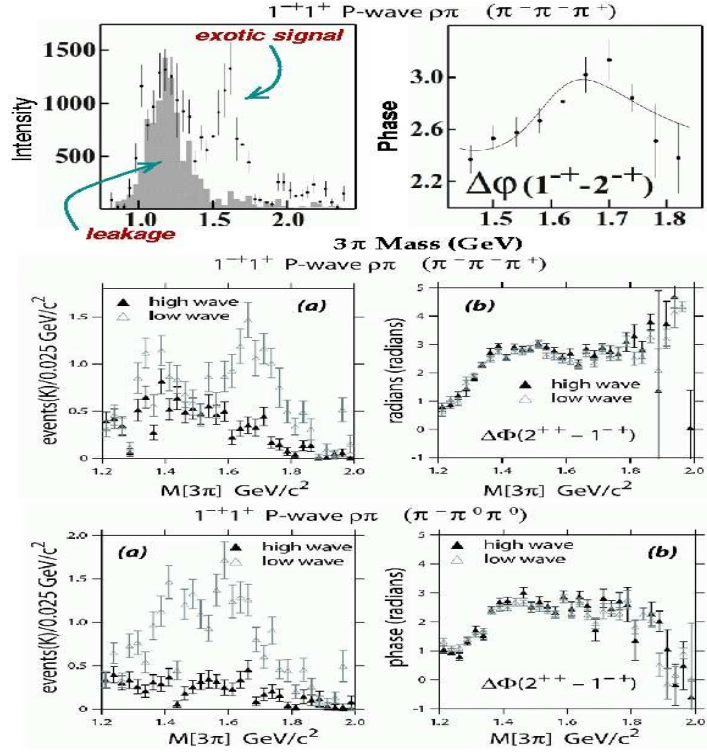


Figure 4. PWA results from analysis of E852 data for the $\pi^-\pi^-\pi^+$ channel (top and middle rows) and for the $\pi^-\pi^0\pi^0$ channel (bottom row) as a function of the 3π effective mass. The upper row of plots is from Ref. [22] and the bottom two rows are from Ref. [27].

the P -wave strength is the dominant signal in $\eta'\pi$ compared to $\rho\pi$. However, the strength in the D -wave used as the phase reference in the $\eta'\pi$ analysis is not well understood. So while there are some noted controversies associated with the $\pi_1(1600)$, there clearly are some tantalizing hints and effects from a number of experiments that need to be further investigated.

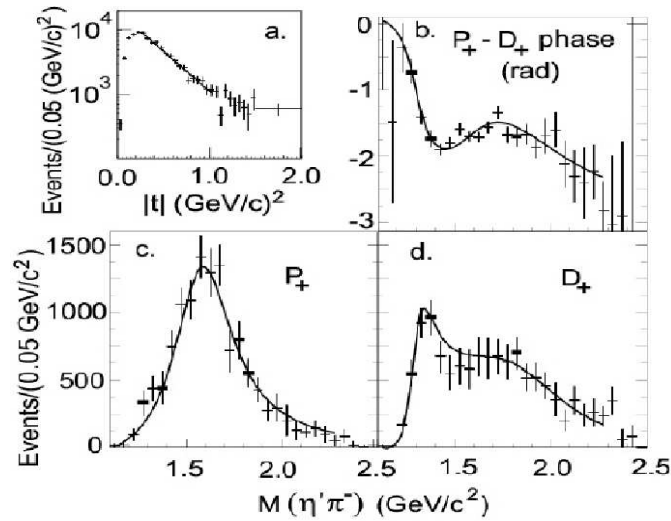


Figure 5. (a) The t -distribution of the $\eta'\pi$ data. (b)-(d) PWA results for the P_+ and D_+ waves as a function of the $\eta'\pi$ effective mass along with the results of a mass-dependent fit [23].

3.3. Evidence for the $\pi_1(2000)$

A final candidate $J^{PC}=1^{-+}$ meson in the literature is the $\pi_1(2000)$ which has been claimed by the E852 Collaboration through its decays into $f_1\pi$ [24] and $b_1\pi$ [25]. While this is encouraging, as this state is more line with what is expected from flux-tube models and the lattice in terms of mass and decay modes, the data are of relatively limited statistical accuracy. In fact the quality of the data is such that strong conclusions regarding the evidence for this state cannot be made.

The reported $\pi_1(2000)$ from $f_1\pi$ was seen through the reaction $\pi^-p \rightarrow \pi^-\pi^-\pi^+\eta n$ (see Fig. 6) and has a mass $M=2001\pm30$ MeV and width $\Gamma=333\pm52$ MeV. As seen from $b_1\pi$ through the reaction $\pi^-p \rightarrow \omega\pi^0\pi^-p$ (see Fig. 7), the mass and width are quoted as $M=2014\pm20$ MeV and $\Gamma=230\pm32$ MeV.

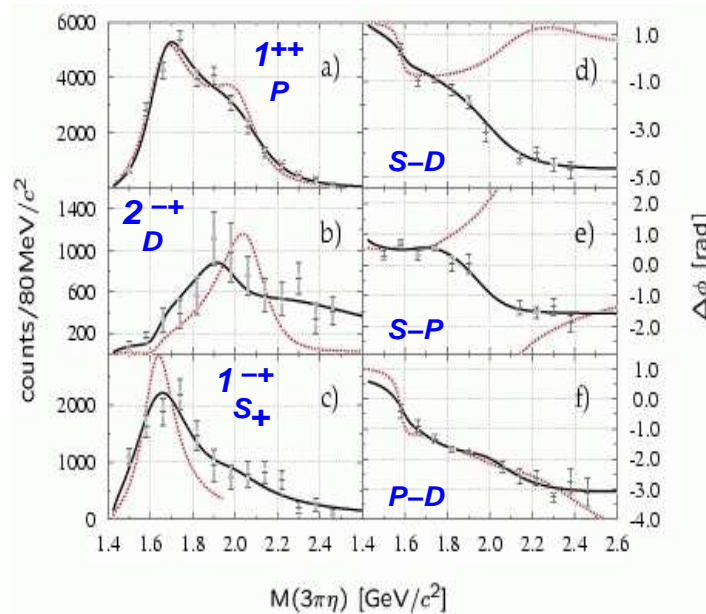


Figure 6. PWA results for the S , P , and D waves as a function of the $f_1\pi$ (or $(3\pi\eta)$) effective mass showing both the intensity and phase difference distributions [24].

4. The Next Generation Experiment

The specifications for the next generation experiment in meson spectroscopy are already quite clear. The essential ingredients are that the detector should be hermetic for both charged and neutral particle final states, with excellent resolution and particle identification capability. This is essential for successful and unambiguous partial wave analysis. The beam energy must be high enough to allow for sufficient phase space for the production of the exotic states, however it should not be too high, otherwise the cross section for background processes will increase and overwhelm the signals that are being sought. The partial wave analysis requires high statistics experiments with sensitivity to production cross sections at the sub-nanobarn level.

In terms of beam properties, the next generation experiment should be carried out with linearly polarized photons. Photon beams are expected to be particularly favorable for the production of exotic hybrids, as the photon sometimes behaves as a virtual vector meson. When the flux tube in this $S=1$ system is excited, both ordinary and exotic J^{PC} are possible. In contrast, for an $S=0$ probe (e.g. pions or kaons), the exotic combinations are not generated. To date, almost all meson spectroscopy experiments in the light-quark sector have been done with incident pion, kaon, or proton probes. High flux photon beams of sufficient quality and energy have not been available, so there are virtually no data on the photoproduction of mesons with masses below 3 GeV. Thus up to now, experimenters have not been able to search for exotic

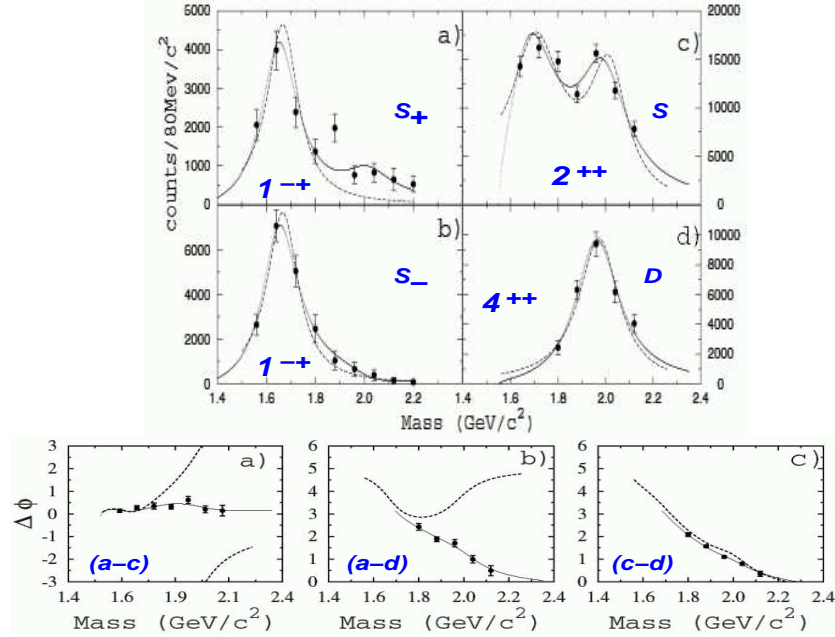


Figure 7. PWA results for the S and D waves as a function of the $b_1\pi$ effective mass showing both the intensity and phase difference distributions [25]. The phase difference plots in the bottom row labeled $(a - c)$, $(a - d)$, and $(c - d)$, refer to the intensity plots labeled as (a) through (d) in the top part of the figure.

hybrid mesons precisely where they are expected. Theoretical calculations indicate that the photoproduction cross sections of light-quark exotic mesons should be comparable to those for conventional meson states in this energy range [28].

As mentioned above, the next generation experiment should employ a linearly polarized photon beam. The diffractive production of a conventional meson takes place via natural parity exchange ($J^P = 0^+, 1^-, 2^+, \dots$) in the intermediate state, whereas exotic meson production takes place via unnatural parity exchange ($J^P = 0^-, 1^+, 2^-, \dots$). Experiments that take place with an unpolarized or a circularly polarized photon beam cannot distinguish between the naturality of the exchanged meson. However with a longitudinally polarized beam, one can distinguish the naturality of the intermediate state by selection based on the angle the polarization vector makes with the hadronic production plane. This capability will be essential in helping to isolate the exotic waves in the data analysis.

5. The Design of the GlueX Experiment

The current Jefferson Laboratory accelerator can deliver electron beams of up to nearly 6 GeV at currents of $\sim 200 \mu\text{A}$ and polarization up to $\sim 80\%$. The planned upgrade of this facility is designed to increase the maximum electron beam energy to 12 GeV, to construct a new experimental Hall, called Hall D, for the GlueX experiment, and to lead to equipment enhancements in the three existing Halls A, B, and C. The current schedule has the 12-GeV facility on track to begin its physics program in 2011-2012.

The GlueX experiment in Hall D has been designed to perform meson spectroscopy over a range of masses up to roughly 3 GeV [29]. Although GlueX aims to investigate the full spectrum of light conventional mesonic states, hybrid and exotic hybrid mesons, glueballs, multi-quark states, and molecular states, the exotic states will be the main initial thrust of the experimental program. Fig. 8 shows a schematic layout of the planned hermetic detector. The photon beam is incident on a liquid-hydrogen target that is located within a large 2 T superconducting solenoidal

magnet. The target is surrounded by drift chambers for charged particle tracking. The tracking system includes a straw tube chamber for tracking at central and backward angles and a series of cathode strip chambers for tracking at forward angles. Both of these packages will also provide for particle identification via dE/dX measurements. Surrounding the tracking detectors is a barrel calorimeter for particle identification and timing. Filling the upstream end of the solenoid will be another calorimeter. Downstream of the magnet is a large time-of-flight array, a Čerenkov detector for particle identification, and a large lead-glass array that forms an electromagnetic calorimeter.

The solenoidal geometry is ideally suited for a high-flux photon beam. The electromagnetic charged particle background (electron-positron pairs) from interactions in the target is contained along the beam line by the axial field of the magnet. The GlueX spectrometer has been designed for large and uniform acceptance for both charged and neutral particle final states, while providing the requisite resolution and particle identification capabilities for spectroscopy.

The GlueX photon beam will be produced using the coherent bremsstrahlung technique. Here the 12 GeV electron beam will impinge on a thin diamond crystal and will produce a linearly polarized beam of 9 GeV photons after collimation. At the target the photon will achieve an average degree of linear polarization in the coherent peak of roughly 40%. This detector system, along with the high duty factor of the electron beam from the accelerator make the search for hybrid mesons quite feasible. GlueX will collect enough data in its first year of operation with photon fluxes of 10^7 to 10^8 s⁻¹ to exceed existing photoproduction data by several orders of magnitude.

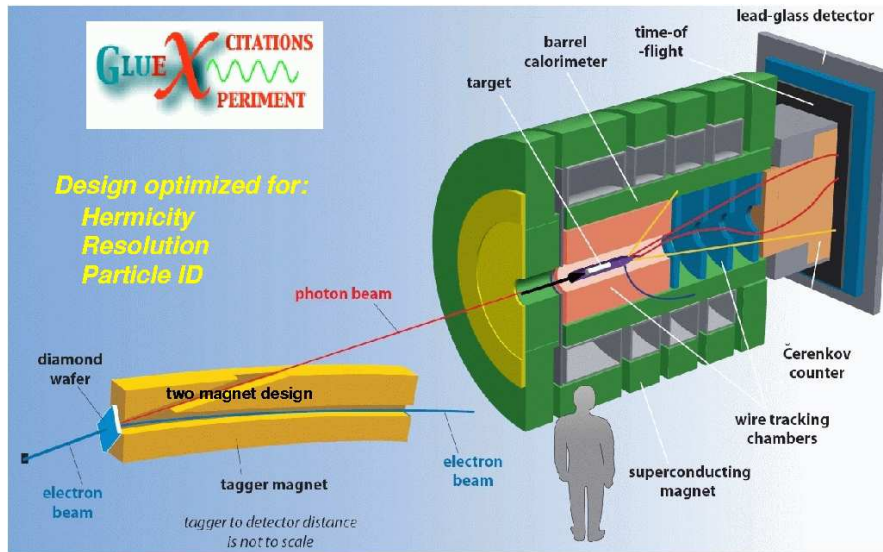


Figure 8. Schematic picture of the GlueX detector and coherent bremsstrahlung photon tagging facility. The subsystems within the solenoid are indicated.

Hand in hand with the design of the experimental equipment, the GlueX Collaboration is performing detailed Monte Carlo studies of the physics, not only to test and improve the design of the spectrometer, but also to develop the software tools essential for the success of the data analysis. The performance of the detector, the beam flux, and the linear polarization of the photon beam determine the level of sensitivity for mapping the hybrid spectrum. The detector acceptance has been designed to be high and uniform in the relevant meson decay angles in the Gottfried-Jackson frame for *both* charged and neutral particle final states. A program of double-blind Monte Carlo studies have been carried out using the GlueX partial wave analysis software. These studies have shown that low-level exotic signals (at the few percent level) can

be successfully pulled out from the data, even with relatively low statistics. Even with extreme distortions in these simulations, leakage effects due to the spectrometer are no more than 1%. To further certify the PWA codes, consistency checks with Monte Carlo and real data will be made among different final states for the same decay mode.

6. Summary and Conclusions

Understanding confinement requires an understanding of the glue that binds quarks into hadrons. Hybrid mesons are perhaps the most promising laboratory to study the nature of the glue. However, since their first observation, their existence has been controversial, but a number of experimental results have provided tantalizing hints for the existence of these mesons. Future studies, such as will be performed with the GlueX experiment at JLab, provide the hope for improved experimental results and interpretations. Here photoproduction promises to be rich in hybrids, starting with those having exotic quantum numbers where little or no data exist. The GlueX experiment that will take place at the energy-upgraded Jefferson Laboratory, will employ photon beams of the necessary flux, duty factor, and polarization, along with an optimized state-of-the-art detector. This experiment will provide for the detailed spectroscopy necessary to map out the hybrid meson spectrum, which is essential for an understanding of the confinement mechanism and the nature of the gluon in QCD.

The author thanks the workshop organizers for the opportunity to discuss the field of exotic meson spectroscopy. He also gratefully acknowledges his fellow GlueX collaborators for their support and many efforts on the experiment to this point in time. This work is supported by the National Science Foundation and the U.S. Department of Energy.

- [1] G.S. Bali, K. Schilling, and C. Schlichter, Phys. Rev. D **51**, 5165 (1995).
- [2] G.S. Bali *et al.*, Phys. Rev. D **62**, 054503 (2000).
- [3] N. Isgur and J. Paton, Phys. Rev. D **31**, 2910 (1985).
- [4] T. Barnes, F.E. Close, and F. de Viron, Nucl. Phys. B **224**, 241 (1983).
- [5] M. Chanowitz and S. Sharpe, Nucl. Phys. B **222**, 211 (1983).
- [6] I.I. Balitsky, D.I. Diakonov and A.V. Yung, Z Phys. C **33**, 265 (1986).
- [7] M.S. Cook and H.R. Fiebig, Phys. Rev. D **74**, 034509 (2006).
- [8] N. Isgur, R. Kokoski, and J. Paton, Phys. Rev. Lett. **54**, 869 (1985).
- [9] M. Tanimoto, Phys. Rev. D **27**, 2648 (1983).
- [10] C. Michael, hep-lat/0302001, (2003).
- [11] J. Dudek, private communication. See contribution to this proceedings.
- [12] D. Alde *et al.*, Phys. Lett. B **205**, 397 (1988).
- [13] I.G. Aznauryan, Z. Phys. C **68**, 459 (1995).
- [14] Y.D. Prokoshkin and S.A. Sadovsky, Phys. Atom. Nucl. **58**, 606 (1995).
- [15] G.M. Beladidze *et al.*, Phys. Lett. B **313**, 276 (1993).
- [16] H. Aoyagi *et al.*, Phys. Lett. B **314**, 246 (1993).
- [17] D.R. Thompson *et al.*, Phys. Rev. Lett. **79**, 1630 (1997).
- [18] A. Abele *et al.*, Phys. Lett. B **423**, 175 (1998); Phys. Lett. B **446**, 349 (1998).
- [19] Particle Data Group, Phys. Rev. D **66**, 1 (2002).
- [20] A.P. Szczepaniak *et al.*, Phys. Rev. Lett. **91**, 092002 (2003).
- [21] A.R. Dzierba *et al.*, Phys. Rev. D **67**, 094015 (2003).
- [22] G.S. Adams *et al.*, Phys. Rev. Lett. **81**, 5760 (1998).
- [23] E.I. Ivanov *et al.*, Phys. Rev. Lett. **86**, 3977 (2001).
- [24] J. Kuhn *et al.*, Phys. Lett. B **595**, 109 (2004).
- [25] M. Lu *et al.*, Phys. Rev. Lett. **94**, 032002 (2005).
- [26] Y. Khokhlov *et al.*, Nucl. Phys. A **663**, 596 (2000).
- [27] A. Dzierba *et al.*, Phys. Rev. D **73**, 072001 (2006).
- [28] A.P. Szczepaniak and M. Swat, Phys. Lett. B **516**, 72 (2001).
- [29] GlueX Collaboration homepage: <http://dustbunny.physics.indiana.edu/HallD/>.